MICROSTRUCTURE CHARACTERISTICS OF CP STEEL AND TRIP STEEL LASER WELDED JOINTS

ŠVEC Pavol, SCHREK Alexander

Slovak University of Technology in Bratislava, Bratislava, Slovakia, EU

Abstract

The microstructures of complex phase 780C steel and TRIP 690T steel joints with thickness of 1.5 mm welded using fibre laser process were evaluated. The microstructures and microhardness of butt joints were characterized in the fusion zones and heat affected zones. The microstructures in the fusion zones were predominantly built of martensite and lower bainite. In both heat affected zones near 780C steel and near 690T steel grain coarsening of dominantly martensitic microstructure with small portion of lower bainite and retained austenite was observed. The microhardness increased in the fusion zone and both heat affected zones of joints. The highest microhardness of 485 $HV_{0.1}$ was measured in the heat affected zone near 780C steel region of joint. The average tensile strength of all joints was 750 MPa and it achieved the strength of the 690T steel, because the failures during the tests occurred in this steel base material.

Keywords: Complex phase steel, TRIP steel, microstructure, microhardness, fibre laser welding

1. INTRODUCTION

Advanced high strength steels (AHSS) with zinc coatings are widely used for tailor welded blanks (TWBs) in automotive industry. Frames, crossbeams, vertical beams, side impact beams, and safety elements are often made of TWBs consisted of AHSS steels such as high strength low alloyed steels, dual phase steels, complex phase (CP) steels, TRIP steel, TWIP steels, etc. The TWBs welded of CP and TRIP steels have increased applications due to their excellent properties. The superior mechanical properties in comparison with standard steels enable the use of thin-walled sections of these steels in modern car bodies, significantly reducing the weight of a vehicle without compromising other attributes such as safety, performance, recyclability and cost. They have moderate price and they possess excellent weldability and formability [1-5]. The significant advantage of CP steels is their complex microstructure consisted of ferritic matrix with bainite and tempered martensite and which is the consequence of high strength with sufficient formability of CP steel sheets. The crucial advantage of TRIP steels is their strain induced transformation of retained austenite into martensite. This transformation, which takes place during the sheet forming, can be exploit when making sections of highly complicated shapes enabling the safety improvement by increasing the amount of absorbed collision energy [5-9].

The fibre lasers have found many applications in car body manufacturing because of their excellent beam quality. Low heat input is important characteristic of laser welding and it is the consequence of small fusion zone (FZ) and heat-affected zone (HAZ) and the lover cost and greater flexibility compared to other welding methods [7-11]. Microstructure changes accompanying the laser welding increase the strength in weld region of TWBs but also worsens their formability. The proper microstructure assures proper ratio between strength and formability. The microstructure is affected mainly by chemical composition of base materials, sheets thicknesses and welding parameters such as power input, welding speed and others. The final microstructure in FZ and HAZ is consequence of rapid heating and cooling cycles. FZ and HAZ are characterised by increased hardness and decreased plastic properties [11-13]. Therefore, it is important to study the transformations taking place in the microstructure of steels subjected to laser welding with concentration on the weldability of TWBs made of CP and TRIP steels.

2. EXPERIMENT

The sheets of CP steel 780C and TRIP steel 690T with thickness of 1.5 mm and zinc coating of 100 g / m^{-2} were used for experiments. The maximal concentration of alloying elements in the experimental steels is given in **Table 1** and their mechanical properties are compared in **Table 2**. Used steels differ in contents of alloying elements. The 690T steel has higher concentration of carbon and manganese, but lower content of chromium and molybdenum compared to 780C steel. In TWBs made of experimental steels, the CP steel 780C can assignee the higher strength and the TRIP steel 690T can assignee deformation zone because of its better formability.

Table 1 Maximal concentration (wt. %) of alloying elements in experimental steels

Steel	C	Mn	Si	Al	P	S	V	B	Cr + Mo	Nb + Ti
780C	0.18	2.2	0.8	2.0	0.08	0.015	0.2	0.005	1.0	0.15
690T	0.32	2.5	2.2	2.0	0.12	0.015	0.2	0.005	0.60	0.20

Table 2 Mechanical properties of experimental steels

Steel	Tensile strength (MPa)	Proof strength (MPa)	Elongation (%)
780C	min. 780	500 - 700	min. 10
690T	min. 690	430 - 550	min. 23

The experimental steel sheets were butt welded using the solid-state fibre laser IPG YLS-500 with maximum output of 5 kW, wave length of 1060 nm and fibre diameter of 100 μm and with the welding head PRECITEC YW52 at the distance of 250 mm from the welded sheets. Welding experiments were conducted on sheets with length of 200 mm and width of 100 mm along the longitudinal edge, which was milled before welding. The butt joints were welded without filler metal at beam powers in the interval from 0.75 kW to 5.0 kW and welding speeds in the interval from 10 mm / s^{-1} to 120 mm / s^{-1}.

The microstructure was studied on samples cut off the welding joints and prepared using standard metallographic techniques. The microstructure was observed using Axiovert 40MAT light microscope and JEOL JSM-IT300 scanning electron microscope (SEM). Energy-dispersive spectroscopy (EDS) was employed for chemical analysis of particular phases. Image analysis was used to measure grain sizes. Microhardness surveys were performed on transverse sections of weld bead centres parallel to the surfaces of sheets using Vickers indenter with load of 100 g. The samples for tensile tests were prepared from welded joints and tests were carried out using universal testing machine Instron 195 at room temperature and the crosshead speed of 10 mm / min^{-1}.

3. RESULTS

The cross section of joint welded at the beam power of 3400 W and the welding speed of 70 mm / s^{-1} can be seen in **Figure 1**. The FZ has wine glass shape typical for laser welding with thickness approximately from 1.0 to 1.3 mm and the largest width at the face and the root region of joint but the lowest one in the centre of joint. Both interfaces of HAZs with base metals (BMs) have narrow shape. The 780C steel BM is on the left and the 690T steel BM is on right in **Figure 1**. The HAZ near 780C CP steel with thickness from 0.4 to 0.7 mm is between the FZ and 780C steel BM and the HAZ near 690T TRIP steel BM with thickness from 0.4 to 0.7 mm is between the FZ and 690T steel. The thicknesses of particular sub zones (FZ, HAZ near 780 C steel, HAZ near 690T steel) decreased with increase of beam power and welding speed. The joint is without porosity, cracks, but with the slight concavity of the face and root sagging. The grain size in both HAZs decreases with the distance from the weld boundaries with the largest grains (coarse grained region) observed in the vicinity of the FZ.

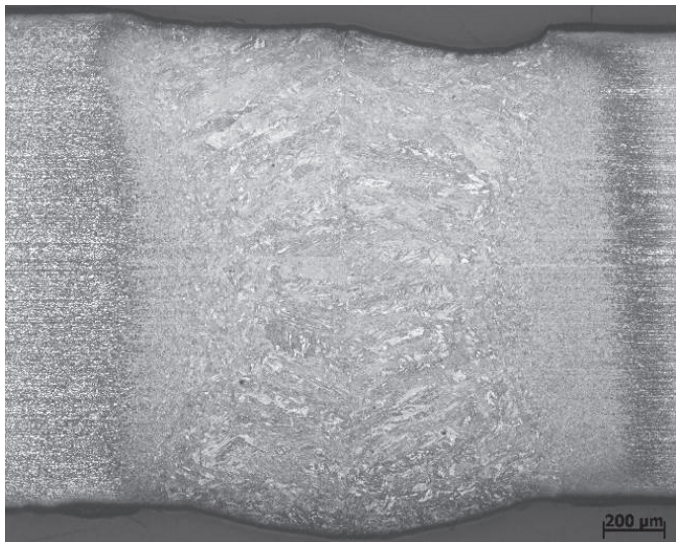

Figure 1 Macrostructure of welded joint of 780C steel with 690T steel

When studying the microstructure evolution in particular sub zones of joints, the both BMs were observed and are documented in **Figures 2** and **3**. The microstructure characteristics of FZ and in coarse grained regions of HAZs are documented from **Figures 4** to **6**.

The SEM micrograph revealing the microstructure of CP steel 780C is documented in **Figure 2**. The microstructure consists of ferrite matrix and rows of martensite and tempered martensite. Ferrite grains are characterised by slight crystallographic texture and heterogeneity in grain size in the interval from 2 to 15 μm. Martensite has the lath morphology and tempered martensite has acicular morphology. Secondary M_3C, M_2C and MC carbides precipitated at the grain boundaries of acicular grains and inside the grains were identified by EDS analysis.

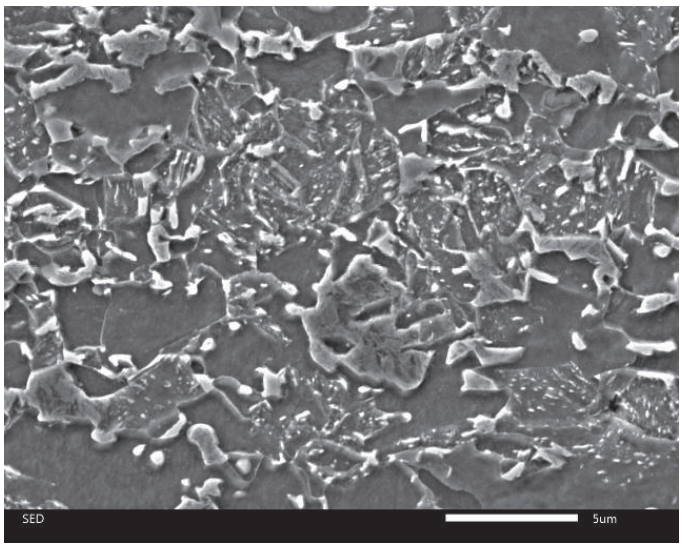

Figure 2 Microstructure of CP steel 780C

The SEM micrograph revealing microstructure of TRIP steel 690T is documented in **Figure 3**. The microstructure of TRIP steel is built by equiaxed ferritic grains with slight crystallographic texture and grain size from 1 to 8 μm and rows of martensite. Occasionally precipitated M_3C carbides were identified by EDS analysis insides the grains.

The microstructure in FZ consisted of coarse columnar dendritic grains oriented perpendicular to the fusion boundary (**Figure 1**). The microstructure of FZ was predominantly built of martensite and lower bainite. Morphological characteristics of low carbon martensite with martensite lath packets can be seen in **Figure 4**.

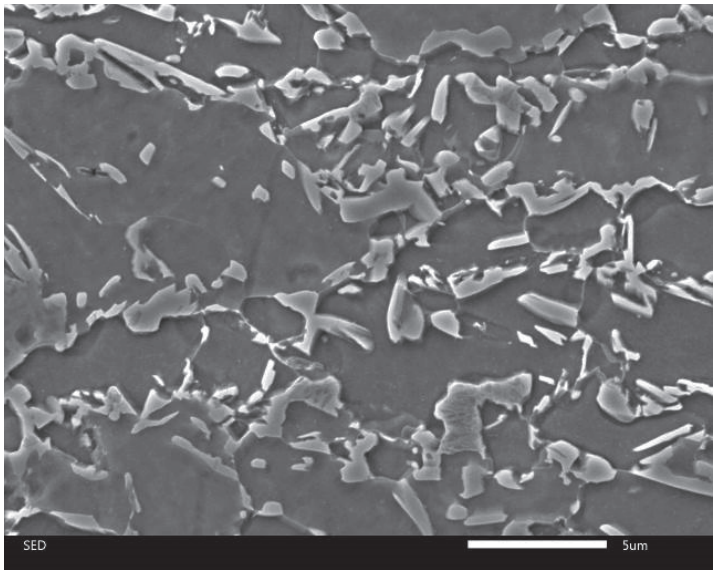

Figure 3 Microstructure of TRIP steel 690T

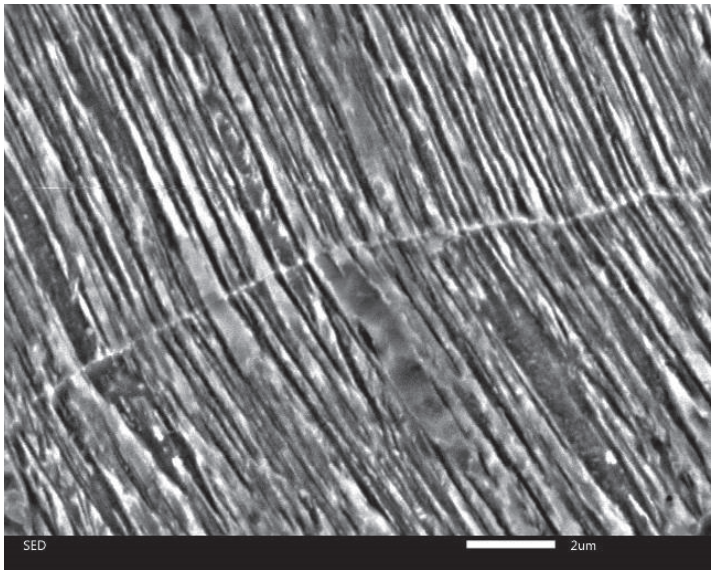

Figure 4 Lath morphology microstructure in FZ of the weld

In the coarse grained high tempered HAZ near 780C steel grain coarsening of former austenitic grain with grain size in the interval from 15 to 30 μm was observed. The microstructure consisted mainly of martensite and lower bainite with occasionally crated small areas of upper bainite and retained austenite, at which grain boundary small M_3C carbides were identified by EDS analysis. Dominant martensitic microstructure with small portion of lower bainite can be seen in **Figure 5**. The microstructure was predominantly built of martensite and lower bainite in the fine grained region of HAZ near 780C steel.

The coarse grained high tempered HAZ near 690T steel in **Figure 6** was characterized by coarsening of former austenitic grain with grain size in the interval from 15 to 25 μm. The microstructure consisted mainly of martensite and small portion of lower bainite and retained austenite. The microstructural characteristic

changed with decreasing of maximal temperature peak during the welding process, so with the distance from the weld. In the region, tightly above the A_3 temperature, which corresponds to the complete transformation to austenite, the microstructure consisted of martensite and ferrite and ferrite portion increased with decreasing of the maximal temperature reached during the welding process. The microstructure in low tempered region of HAZ was characterized by finer grain of martensite and ferrite.

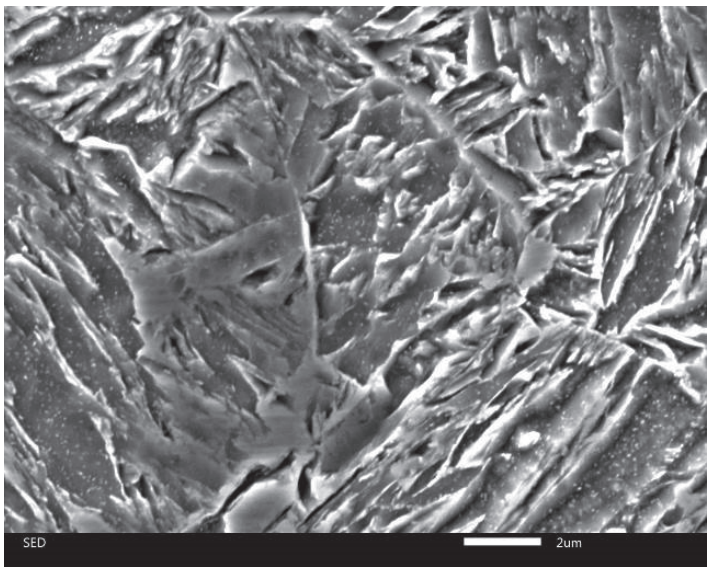

Figure 5 Martensite and lower bainite in coarse grained region of HAZ near 780C steel

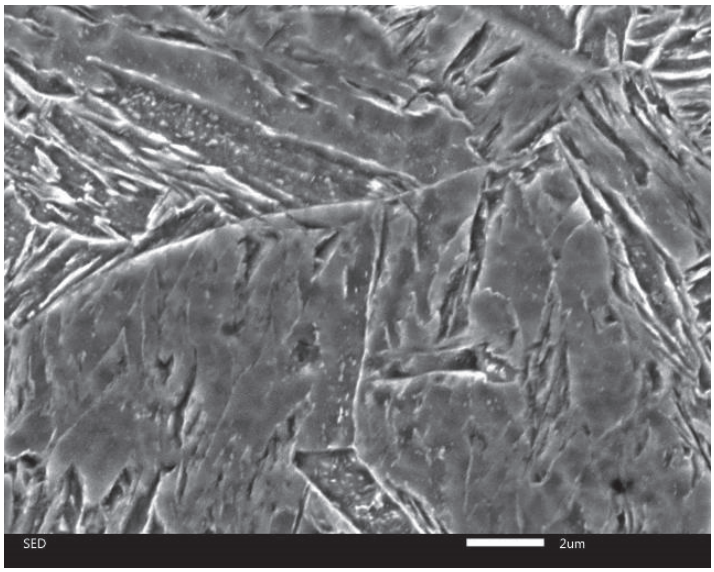

Figure 6 Martensite and lower bainite in coarse grained region of HAZ near 690T steel

The microhardness profile across the FZ, HAZs and BMs was characterized with increased microhardness values in both HAZs from BMs towards the FZ. The hardness of 780C steel BM was in interval from 263 to 281 $HV_{0.1}$ and with average value of 271 $HV_{0.1}$ and this value represents complex microstructure of CP steel. However, the microhardness in interval from 228 to 251 $HV_{0.1}$ and with average value of 239 $HV_{0.1}$ measured for 690T steel represents a ferritic-martensitic microstructure of the TRIP steel. The microhardness values in FZ were in interval from 342 to 428 $HV_{0.1}$. The microhardness in HAZ near 780C steel was in interval from 254 to 485 $HV_{0.1}$ and the microhardness in HAZ near 690T steel was from 220 to 457 HV0.1. The value of 485 $HV_{0.1}$ was the highest measured microhardness and it was measured in coarse grained region of HAZ near

780C steel. The smallest value in the HAZ near 780C steel was 254 $HV_{0.1}$ and was measured in vicinity of 780C steel BM and represents the softening region. Similar softening region in HAZ near 690T steel represents the value of 220 $HV_{0.1}$ which was the smallest value in this HAZ.

The tensile tests showed the average weld metal strength of 750 MPa and an apparent average elongation of 17.5 %. The weld strength was higher than the tensile strength of weaker 690T steel and all samples broke in 690T TRIP steel BM.

4. CONCLUSIONS

The fibre laser welding of complex phase steel 780C with TRIP steel 690T was studied with concentration on microstructure, microhardness and tensile strength. The joints welded using a fibre laser with different input power and welding speed were free of microscopical defects.

The microstructure in the FZ was predominantly built by the lath of martesite and lower bainite which were built in packets within large columnar grains. The microstructures in coarse grained region of HAZ near 780C steel consisted of martensite and lower bainite. Martensite, lower bainite and reatained austenite were observed in coarse grained region of HAZ near 690T steel. The microstructure consisted of martensite and ferrite in fine grained region of HAZ near 690T steel. The ferrite portion increased with increased distance from the weld and decreasing of the maximal temperature reached during the welding process.

Microhardness profiles across the welded joints were characterized with increased microhardness values in FZ and both HAZs. The maximum microhardness was measured within the HAZ near 780C steel with the value of 485 $HV_{0.1}$. The maximal hardness in the HAZ near 690T steel reached 457 $HV_{0.1}$. The hardness in the FZ was in interval from 342 to 428 $HV_{0.1}$. The average tensile strength of the fibre laser welded joints was 750 MPa and it reached the strength of the 690T steel with all welded specimens failing in this steel.

ACKNOWLEDGEMENTS

This work was supported by the Slovak Research and Development Agency under the contract No. APVV-0281-12

REFERENCES

[1] HONG, K. M., SHIN, Y. C. Prospects of laser welding technology in the automotive industry: A review. *Journal of Materials Processing Technology*, 2017, vol. 245, pp. 46-69.

[2] GRAJCAR, A., MORAWIECA, M., ROZANSKIB, M., STANO, S. Twin-spot laser welding of advanced high-strength multiphase microstructure steel. *Optics & Laser Technology*, 2017, vol. 92, pp. 52-61.

[3] SHARMA, R. S., MOLIAN, P. Yb:YAG laser welding of TRIP780 steel with dual phase and mild steels for use in tailor welded blanks. *Materials and Design*, 2009, vol. 30, no. 10 pp. 4146-4166.

[4] RAMESH, M. V. L., RAO, P.S., RAO, V. V., PRABHAKAR, V. P. Structure - Properties in Laser Beam Welds of High Strength Low Alloy Steel. *Materials Today: Proceedings*, 2015, vol. 2, no. 4-5, pp. 2532-2537.

[5] REISGEN, U., SCHLESER, M., MOKROV, O., AHMED, E. Statistical modelling of laser welding of DP/TRIP steel sheets. *Optics & Laser Technology*, 2012, vol. 44, no. 1, pp. 92-101.

[6] NI, J., LI, Z., HUANG, J., WU, Y. Strengthening behavior of weld metal of laser hybrid welding for microalloyed steel. *Materials and Design*, 2010, vol. 31, no. 10 pp. 4876-4880.

[7] ZHAO, L., WIBOWO, M. K., MERMENS, M. J. M., BOHEMEN, S. M. C., SIETSMA, J. Retention of austenite in the welded microstructure of a 0.16C-1.6Mn-1.5Si (wt. %) TRIP steel. *Journal of Materials Processing Technology*, 2009, vol. 209, no. 10, pp. 5286-5292.

[8] WANG, X. N., CHEN, C. J., WANG, H. S., ZHANG, S. H., ZHANG, M., LUO, X. Microstructure formation and precipitation of microalloyed C-Mn steel. *Journal of Materials Processing Technology*, 2009, vol. 209, no. 12-13, pp. 5286-5292.

[9] MUJICA, L., WEBER, S., PINTO, H., THOMY, C., VOLLERTSEN, F. Microstructure and mechanical properties of laser-welded joints of TWIP and TRIP steels. *Materials Science & Engineering A*, 2010, vol. 527, no. 7-8, pp. 2071-2078.

[10] EVIN, E., NÉMETH, S., TOMÁŠ, M. Effect of laser welding on safety characteristics of high strength steel sheets. *Acta Metallurgica Slovaca*, 2015, vol. 21, no. 3, pp. 184-194.

[11] MORAWIEC, M., ROZANSKI, M., GRAJCAR, A., STANO, S. Effect of dual beam laser welding on microstructure-property relationships of hot-rolled complex phase steels. *Archives of civil and mechanical engineering*, 2017, vol. 17, no. 1, pp. 145-153.

[12] VIŇÁŠ, J., ÁBEL, M. Analysis of Laser Welds on Automotive Steel Sheets. *Materials Science Forum*, 2015, vol. 818, pp. 239-242.

[13] MEŠKO, J., ZRAK, A., MULCZYK, K., TOFIL, S. Microstructure analysis of welded joints after laser welding. *Manufacturing Technology*, 2014, vol. 14, no. 3, pp. 355-359.